



HAL
open science

Millennial-scale iceberg discharges in the Irminger Basin during the Last Glacial Period: Relationship with the Heinrich events and environmental settings

Mary Elliot, Laurent Labeyrie, Gerard Bond, Elsa Cortijo, Jean-Louis Turon, Nadine Tisnerat, Jean-Claude Duplessy

► To cite this version:

Mary Elliot, Laurent Labeyrie, Gerard Bond, Elsa Cortijo, Jean-Louis Turon, et al.. Millennial-scale iceberg discharges in the Irminger Basin during the Last Glacial Period: Relationship with the Heinrich events and environmental settings. *Paleoceanography*, 1998, 13 (5), pp.433-446. 10.1029/98PA01792 . hal-02497216

HAL Id: hal-02497216

<https://hal.science/hal-02497216>

Submitted on 9 Oct 2020

HAL is a multi-disciplinary open access archive for the deposit and dissemination of scientific research documents, whether they are published or not. The documents may come from teaching and research institutions in France or abroad, or from public or private research centers.

L'archive ouverte pluridisciplinaire **HAL**, est destinée au dépôt et à la diffusion de documents scientifiques de niveau recherche, publiés ou non, émanant des établissements d'enseignement et de recherche français ou étrangers, des laboratoires publics ou privés.

Millennial-scale iceberg discharges in the Irminger Basin during the last glacial period: Relationship with the Heinrich events and environmental settings

Mary Elliot,¹ Laurent Labeyrie,^{1,4} Gerard Bond,² Elsa Cortijo,¹ Jean-Louis Turon,³ Nadine Tisnerat,¹ and Jean-Claude Duplessy¹

Abstract. High-resolution records of coarse lithic content and oxygen isotope have been obtained in a piston core from the Irminger Basin. The last glacial period is characterized by numerous periods of increased iceberg discharges originating partly from Iceland and corresponding to millennial-scale instabilities of the coastal ice sheets and ice shelves in the Nordic area. A comparison with midlatitude sediment cores shows that ice-rafted material corresponding to the Heinrich events was deposited synchronously from 40° to 60°N. There are thus two oscillating systems: every 5-10 kyr massive iceberg armadas are released from large continental ice caps, whereas more frequent instabilities of the coastal ice sheets in the high latitude regions occur every 1.2-3.8 kyr. At the time of the Heinrich events the synchronicity of the response from all the northern hemisphere ice sheets attests the existence of strong interactions between the two systems.

1. Introduction

Major climatic anomalies related to periods of massive iceberg discharges have punctuated the last glacial period, from 10 to 60 ka. In the North Atlantic sediment cores these events are characterized by sudden increases in the coarse lithic fraction (>150 μm), reduced foraminiferal fluxes, and a lowering of sea surface salinities: the Heinrich events (HE) [Heinrich, 1988; Bond *et al.*, 1992, 1993; Bond and Lotti, 1995; Labeyrie *et al.*, 1995; Maslin *et al.*, 1995; Cortijo *et al.*, 1997]. The presence of detrital carbonate within the lithic layers and the geochemical signature of the noncarbonate fraction has led to the conclusion that the major source of icebergs during these events was the Laurentide ice sheet [Andrews and Tedesco, 1992; Bond *et al.*, 1992; Grousset *et al.*, 1993; Bond and Lotti, 1995; Bischof *et al.*, 1996; Gwiazda *et al.*, 1996a, b]. Model results stipulate that the accumulation of heat at the base of the Laurentide ice sheet, released by the geothermal heat flux, was sufficient to periodically create a disequilibrium of the ice cap and lead to sudden increases in iceberg discharges [MacAyeal, 1993a, b]. However, if all the northern hemisphere ice sheets synchronously released iceberg armadas, then a more global mechanism [Denton *et al.*, 1986; Bond and Lotti, 1995] or rapid interaction between the ice sheets would be necessary to explain these events. These links could operate through changes of the ice shelf dynamics [Hulbe, 1997] due to changes in sea level or surface hydrology.

Furthermore, the air temperature variations derived from the $\delta^{18}\text{O}$ record of the Greenland ice cores reveal, for the same pe-

riod, climate variability on millennium timescales [Dansgaard *et al.*, 1993]. These Dansgaard-Oeschger cycles (D-O) are characterized by rapid warming, leading within a few hundred years to interstadial periods, followed by progressive cooling to stadials. The massive iceberg discharges corresponding to the HE appear to occur during the coldest stadials [Bond *et al.*, 1993; Broecker, 1994; Bond and Lotti, 1995].

A major issue in the general understanding of the Heinrich events is thus whether or not all the northern hemisphere ice caps underwent synchronous iceberg discharges. Most studies which aimed at the reconstruction of the spatial and temporal distribution of these layers have mainly focused on sediment cores from the midlatitudes of the North Atlantic Ocean (40°-55°N) where there is a maximum deposition of ice-rafted detritus (IRD). In the higher latitudes of the North Atlantic the presence of major IRD deposits corresponding to the Heinrich events has not yet been clearly established.

The aim of this study is thus to reconstruct the history of iceberg discharges from the high-latitude regions of the North Atlantic Ocean, to define their sedimentary signature, and to determine their impact on the hydrology of surface waters. The Irminger Basin is the major passage for icebergs drifting from the Greenland, Norwegian, and Arctic Seas into the Atlantic Ocean and is thus ideally located for estimating the glacial iceberg fluxes from these regions, which we will refer to as the "Nordic Regions" hereafter. Ice-rafted lithics from this area can originate from Greenland, Iceland, the Faeroe Islands, Fennoscandinavia, and the other continental masses which surround the Nordic Seas. Furthermore, the proximity of this oceanic basin to the Greenland ice cap, where rapid temperature oscillations have been recorded, also gives the opportunity to study the millennium timescale climatic oscillations. A high-resolution record of the coarse lithic content (>150 μm), the planktonic foraminiferal abundance, and oxygen isotopes has been obtained from sediment core SU 90-24 (62°40'N, 37°22'W, 2085 m) from the Irminger Basin (Figure 1). Accelerator mass spectrometry (AMS) ^{14}C dates are used to constrain the age scale and provide the possibility to test the synchronicity of the iceberg discharges that punctuated the last glacial period. The results will then be closely compared to other sediment

¹Laboratoire des Sciences du Climat et de l'Environnement, Laboratoire mixte CNRS-CEA, Gif sur Yvette, France.

²Lamont-Doherty Earth Observatory, Palisades, New York.

³Département de Géologie et Océanographie, CNRS Unité de Recherche Associé, Talence, France.

⁴Also at Département des Sciences de la Terre, Université Paris-sud Orsay, Orsay cedex France.

Copyright 1998 by the American Geophysical Union.

Paper number 98PA01792.
0883-8305/98/98PA-01792\$12.00

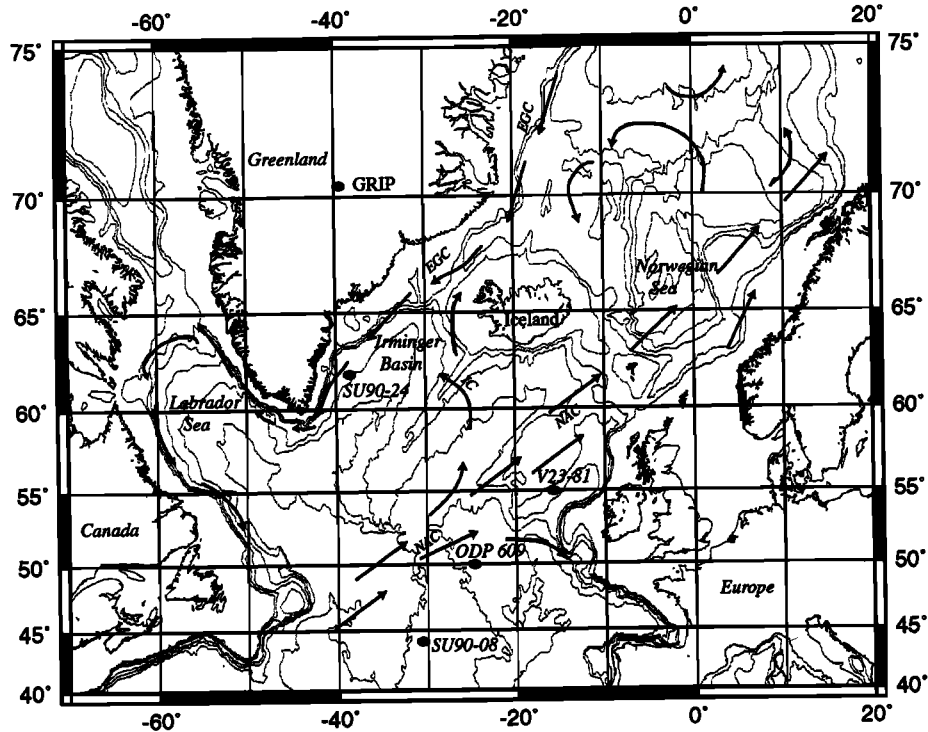


Figure 1. Core location and sea surface currents. NAC, North Atlantic current, IC, Irminger Current and EGC, East Greenland Current. This map was obtained from Weinelt Martin' Online Map Creation, at URL. (version current at March, 24, 1998) <<http://www.aquarius.palaeoz.geomar.de/omc/>>

cores from the midlatitudes of the North Atlantic Ocean: Ocean Drilling Program (ODP) site 609 and core V 23-81 reported by Bond *et al.* [1992, 1993] and Bond and Lotti [1995] and core SU 90-08 by Grousset *et al.* [1993]; Cortijo *et al.* [1997] and Vidal *et al.* [1997] (Figure 1 and Table 1).

2. Methods

2.1. Oxygen Isotope Variations

A detailed oxygen isotope record has been obtained from planktonic foraminifera *Neogloboquadrina pachyderma* left coiling (*N. pachyderma* l.c.) in the 200-250 μm size range. The isotope measurements were performed at the Laboratoire des Sciences de l'Environnement et du Climat in Gif-sur-Yvette using an automated preparation line coupled to a Finnigan MAT 251 mass spectrometer. The mean external reproducibility of powdered carbonate standard is $\pm 0.05\text{‰}$ for oxygen and carbon. Measurements were obtained from samples weighing a minimum of 40 μg corresponding to about seven foraminifera shells. The data are reported as $\delta^{18}\text{O}$ versus Pee Dee belemnite

standard (PDB) after calibration with National Bureau of Standards (NBS)19 [Coplen, 1988; Hut, 1987].

2.2. Lithic and Faunal Counts

The coarse sediment fraction ($>150\ \mu\text{m}$) was counted in order to estimate the ice-rafted detritus input and the planktonic foraminifera assemblages. The samples were spread on a tray subdivided into 45 squares of equal size, a certain number of which were randomly counted. A minimum of 300 planktonic individuals and/or lithic grains were counted. The detrital counts in core SU 90-24 are presented as the number of lithic particles $>150\ \mu\text{m}$ per gram of dry sediment. This parameter is an indicator of the proportion of coarse versus fine sediment fractions. The percentage of detritus versus the total entities in the $>150\ \mu\text{m}$ size range integrates both changes of the IRD and the planktonic foraminifera content [Bond and Lotti, 1995].

Foraminiferal assemblages were used as an indicator of sea surface temperature (SST) variations. The relative percentage of planktonic foraminifera *N. pachyderma* l.c. is commonly used as a sea surface paleotemperature proxy because this planktonic

Table 1. Core Locations, Water Depths, and Average Sedimentation Rates

Core	Latitude	Longitude	Depth	Sedimentation Rates, Location
				cm ka^{-1}
SU 90-24	62°40'N	37°22'W	2100	17 Irminger Basin
V 23-81	54°15'N	16°50'W	2400	13 East Atlantic
ODP 609	49°52'N	24°14'W	3900	6.5 Central-East Atlantic
SU 90-08	43°31'N	30°24'W	3100	6 Central Atlantic

Table 2. The Pointers are the Chronostratigraphic Markers (AMS ^{14}C Dates and Other Age Control Points) Used to Derive the Age Scale of Cores SU 90-24 and SU 90-08 and Ocean Drilling Program (ODP) Site 609 and Core V 23-81

SU 90-24			V 23-81			ODP Site 609			SU 90-08		
Depth, cm	Pointers, ka	2 σ , ka	Depth, cm	Pointers, ka	2 σ , ka	Depth, cm	Pointers, ka	2 σ , ka	Depth, cm	Pointers, ka	2 σ , ka
0	9.8	0.1	157	10.9	0.1	55	11.1		30	7.5	
5	11.0	0.1	205 ^a	12.2 ^a	0.1 ^a	73.5 ^a	12.4 ^a	0.2 ^a	60 ^a	13.0 ^a	0.1 ^a
22	11.4	0.1	219 ^a	13.6 ^a	0.1 ^a	79.5 ^a	13.3 ^a	0.1 ^a	72 ^a	14.8 ^a	0.1 ^a
46 ^a	12.4 ^a	0.2 ^a	221 ^a	14.2 ^a	0.1 ^a	84.5 ^a	14.6 ^a	0.2 ^a	80 ^a	14.9 ^a	0.1 ^a
62 ^a	13.0 ^a	0.2 ^a	223 ^a	14.3 ^a	0.1 ^a	87.5 ^a	16.0 ^a	0.2 ^a	100	18.3	0.2
76 ^a	14.3 ^a	0.2 ^a	227 ^a	14.8 ^a	0.1 ^a	90.5	16.4	0.2	120 ^b	20.7 ^b	0.2 ^b
96 ^a	15.6 ^a	0.2 ^a	229 ^a	15.0 ^a	0.1 ^a	98.5	17.0	0.1	134 ^b	22.1 ^b	0.2 ^b
110	16.5	0.2	251 ^a	15.7 ^a	0.2 ^a	107.5	18.9	0.2	162 ^c	27.1 ^c	0.3 ^c
120	17.9	0.2	263	17.3	0.1	110.5 ^b	20.0 ^b	0.3 ^b	170	29.7	0.5
140 ^b	19.0 ^b	0.2 ^b	274	17.9	0.2	111.5 ^b	20.6 ^b	0.3 ^b	192 ^d	33.5 ^d	0.7 ^d
149 ^b	20.0 ^b	0.2 ^b	287.5	18.3	0.2	112.5 ^b	21.1 ^b	0.2 ^b	210 ^d	35.7 ^d	0.9 ^d
156 ^b	20.2 ^b	0.2 ^b	291	18.4	0.2	115.5 ^b	21.4 ^b	0.2 ^b	252	44.3	*
160 ^b	21.0 ^b	0.3 ^b	321 ^b	20.4 ^b	0.2 ^b	118.5 ^b	22.4 ^b	0.3 ^b	335	59	tr 3/4
174 ^b	22.7 ^b	0.3 ^b	323 ^b	20.5 ^b	0.2 ^b	140.5 ^c	25.3 ^c	0.4 ^c			
206 ^c	25.2 ^c	0.4 ^c	327 ^b	20.6 ^b	0.2 ^b	148.5 ^c	26.2 ^c	0.3 ^c			
210 ^c	25.3 ^c	0.4 ^c	329 ^b	21.0 ^b	0.2 ^b	153.5	29.2	0.7			
214 ^c	25.5 ^c	0.4 ^c	331 ^b	21.2 ^b	0.2 ^b	166.5	30.1	0.7			
240 ^c	26.3 ^c	0.4 ^c	333 ^b	21.7 ^b	0.2 ^b	174.5	30.7	0.7			
280	29.7	0.6	337 ^b	22.0 ^b	0.2 ^b	238.5	35.2	*			
334	31.2	0.6	343 ^b	22.4 ^b	0.2 ^b	277	42.6	*			
392	32.6	0.7	371	24.7	0.2	304	44.6	*			
396 ^d	33.2 ^d	0.8 ^d	381 ^c	26.3 ^c	0.3 ^c	336	50.5	*			
420 ^d	34.1 ^d	0.9 ^d	391 ^c	29.0 ^c	0.3 ^c	349	55	AZII			
460	38.4	1.3	393	29.1	0.3						
470	40.3	1.7	501	35.2	*						
520	44.2	2.6									
750	55	AZII	385 ^e	17.2 ^e	0.1 ^e						
860	59	tr 3/4	421 ^e	27.7 ^e	0.3 ^e						
			339 ^e	21.1 ^e	0.2 ^e						
130 ^e	20.1 ^e	0.2 ^e									
482 ^e	35.7 ^e	1.2 ^e									
500 ^e	34.9 ^e	1.8 ^e									
509 ^e	38.9 ^e	1.8 ^e									
488 ^e	40.5 ^e	2.2 ^e									
498 ^e	44.3 ^e	4.6 ^e									

Data for core SU 90-08 is from Grousset *et al.* [1993], Cortijo *et al.* [1997], and Vidal *et al.* [1997], and data from ODP site 609 and core V 23-81 are from Bond and Lotti [1995] (see Figure 1 and Table 1). The AMS ^{14}C dates have been corrected for a constant surface water reservoir age of 400 years; they are expressed in ka, and the associated 2 σ error bars are also indicated. The other control points obtained by correlation with core SU 90-24 are indicated by asterisks. A certain number of AMS ^{14}C dates were rejected; these dates correspond to the observed age reversals (Figure 2).

^a From Figure 5a.

^b From Figure 5b.

^c From Figure 5c.

^d From Figure 5d.

^e Rejected.

species largely dominates the fauna in the polar waters and is absent in warmer transitional waters [Bé and Tolderlund, 1971; Ruddiman and McIntyre, 1981].

2.3. Age Scale

AMS ^{14}C dates have been obtained on 32 monospecific samples of planktonic foraminifera *N. pachyderma* l.c. in Gif-sur-Yvette (Table 2). A minimum of 10 mg of foraminifera were sampled in order to obtain two measurements per level. Bioturbation effects have been minimized by sampling in the peak abundance [Bard *et al.*, 1994]. A correction of 400 years was applied to correct for surface water reservoir age [Bard, 1988]. The different age scales were not corrected to calendar ages because of the lack of constraint on the initial $^{14}\text{C}/^{12}\text{C}$ ratio for

ages older than 20 ka [Bard *et al.*, 1993] and also because this study is limited to marine records which have all been dated by AMS ^{14}C .

3. Results

3.1. Irminger Basin: Core SU 90-24

The high-resolution oxygen isotope record covers most of marine isotope stages (MIS) 3 and 2 and the base of MIS 1 (Figure 2). This period is punctuated by a series of well-defined light $\delta^{18}\text{O}$ anomalies of 1‰–1.5‰ amplitude similar to those observed in the midlatitudes of the North Atlantic Ocean during the HE [Bond *et al.*, 1992; Grousset *et al.*, 1993; Labeyrie *et al.*, 1995]. Although numerous periods of increased

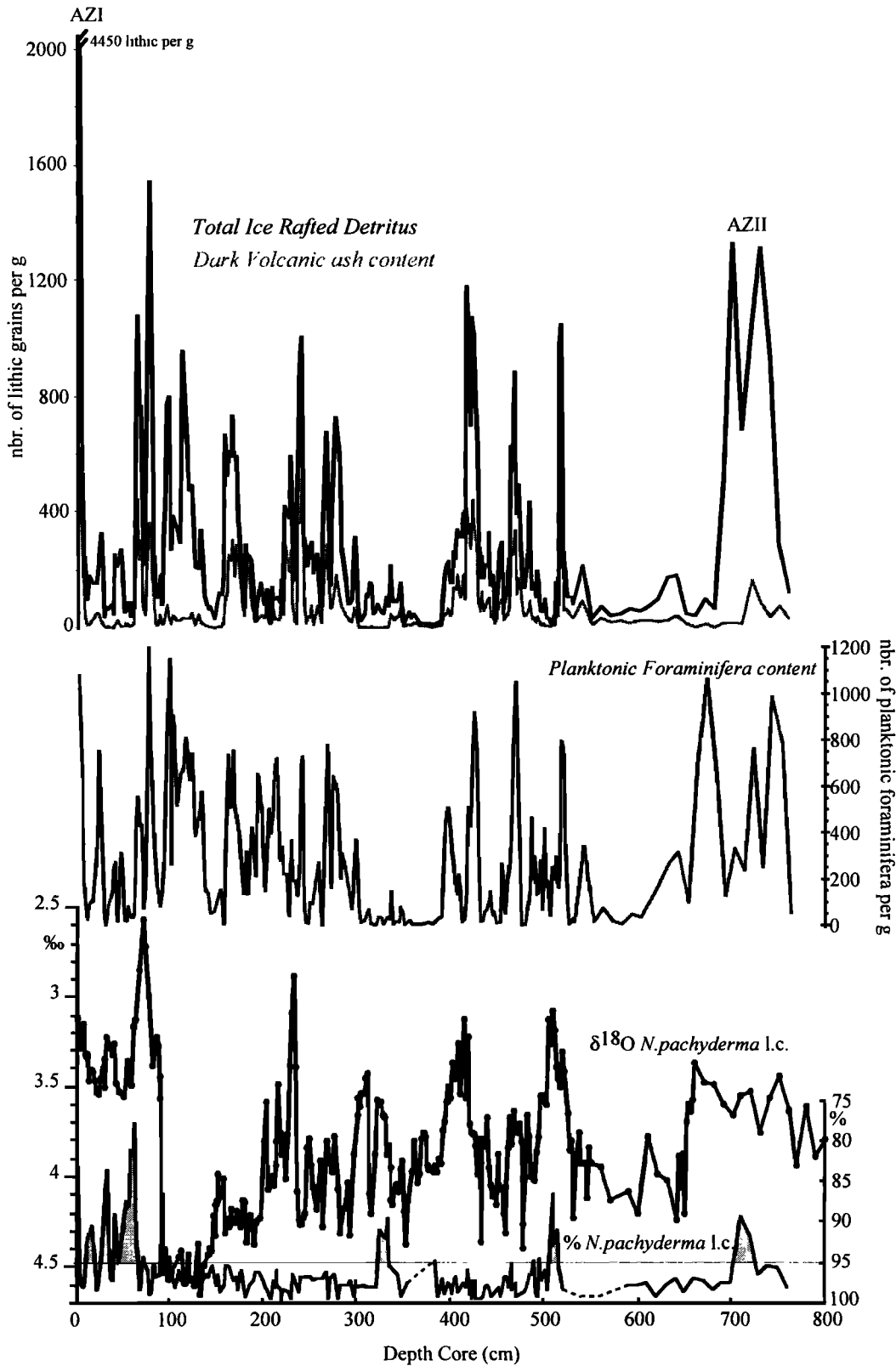


Figure 2. Total coarse lithic counts ($>150\ \mu\text{m}$), coarse dark volcanic ash content, and planktonic foraminiferal abundance per gram of dry sediment. *Neogloboquadrina pachyderma* l.c. oxygen isotope variations and the % *N. pachyderma* l.c. records are expressed in per mill and percent, respectively. All records are from core SU 90-24 and are plotted versus depth. The % *N. pachyderma* l.c. is based on a minimum of 300 individuals except for 80 levels, with low foraminiferal concentration, where between 200 and 300 individuals were counted. Ash zone I (AZI) and ash zone II (AZII) correspond to two thick layers rich in rhyolitic glass which bracket the studied period.

ice-rafted debris input can be observed, only a certain number are associated with the light $\delta^{18}\text{O}$ anomalies (Figure 2). The relationship between these lithic layers and the Heinrich events will only be constrained by an accurate age scale based on AMS ^{14}C dates.

The percentage of *N. pachyderma* l.c. obtained from core SU 90-24 (Figure 2) yields values generally > 95% throughout most of the glaciation. Only a few "warm" events can be observed from 0 to 70 cm and at 320, 510, and 710 cm. Nevertheless, the planktonic foraminiferal abundance is characterized by important variations (Figure 2). Periods of very low foraminiferal abundance can be observed, for example, between 300 and 400 cm depth followed by abrupt and sudden foraminiferal increases which are associated with periods of increased IRD content.

3.2. Age Scale of Core SU 90-24

The age scale of core SU 90-24 has been obtained by linear interpolation between AMS ^{14}C dates and other control points

(Table 2). Ash zone I (AZI) at 5 cm has previously been dated in the ocean sediments at around 11-11.1ka [Bard *et al.*, 1994]. This age is close to the age obtained in core SU 90-24: 11.5 ± 0.12 ka (both ages are not corrected for the 400 year surface water reservoir age). There is one age reversal at 130 cm and significant dating dispersion below 460 cm. These AMS ^{14}C dates will not be taken into consideration, and the age of the lithic events which occur before 35 ka will not be discussed in detail. The position of ash zone II (AZII) at 750 cm has an estimated age of 55 ka [Ruddiman and Glover, 1972], and the limit of marine isotope stage 3/4 at 860 cm dated at 59 ka [Martinson *et al.*, 1987] were used to constrain the sedimentation rate at the base of the core (Figure 3).

3.3. Comparison of the Lithic Events in the Irminger Basin With Midlatitude Sediment Cores

The comparison of the coarse lithic content recorded in a series of sediment cores from 43°N in the Atlantic Ocean to 62°N in the Irminger Basin (Figure 1) from 10 to 60 ka is reported in

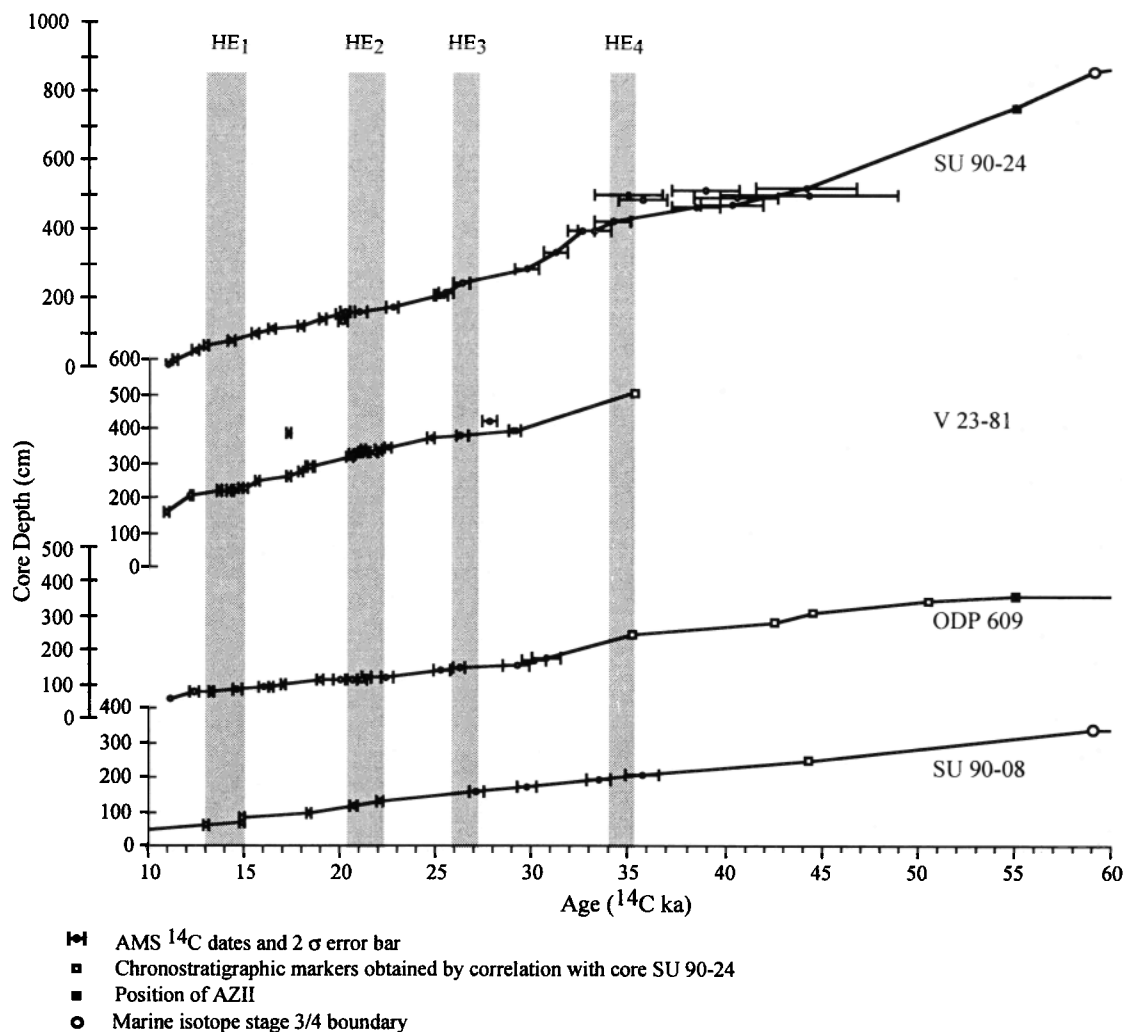


Figure 3. Age scale of core SU 90-24 and other cores presented in this study from 10 to 60 ka. These age scales have been obtained by linear interpolation between the accelerator mass spectrometry (AMS) ^{14}C dates and other stratigraphic control points: AZII at 55 ka and the limit of isotope stage 3/4 at 59 ka. In core SU 90-24, there are some reversals after 35 ka, and these AMS ^{14}C dates were rejected (Table 2). The shaded boxes indicate the average age and duration of Heinrich events (HE₁ to HE₄) and the extrapolated age of HE₅, obtained from this study (see Table 3).

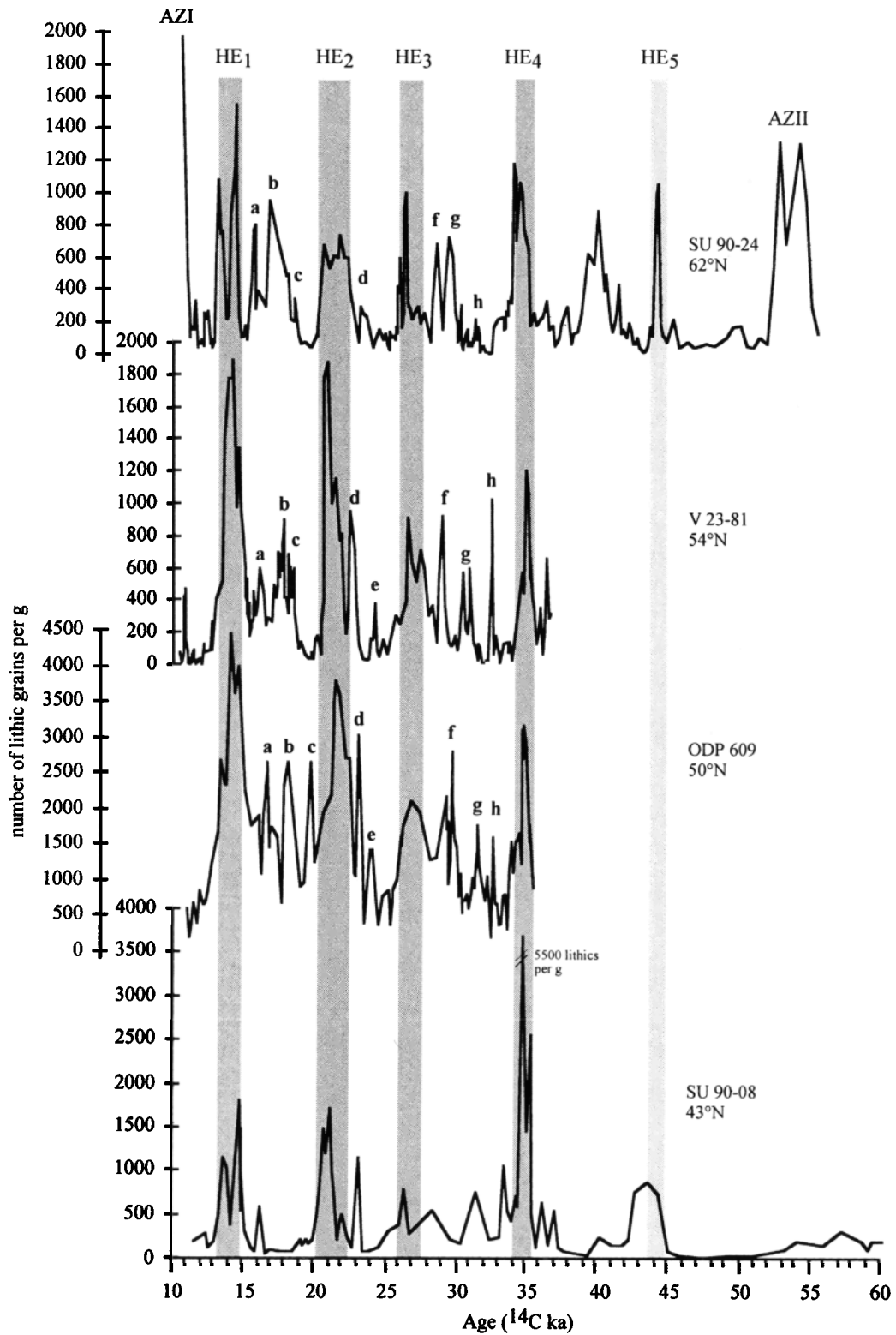


Figure 4. Results obtained from a series of sediment cores taken from 43°N in the North Atlantic Ocean to 62°N in the Irminger Basin. The shaded intervals indicate the average age and duration of HE₁ to HE₄, obtained from this study (see Table 3) and the extrapolated age of HE₅ (45 ka). The positions of the HE₁ to HE₅ have previously been identified in ODP site 609 and core SU 90-08 [Bond et al., 1993; Grousset et al., Cortijo et al., 1997; 1993; Vidal et al., 1997]. Lithic layers in core SU 90-24 can be correlated to these detrital events. Other lithic events have been labeled a-h [Bond and Lotti, 1995]; they can also be observed at 62°N.

Figure 4. The age scale of each core has been obtained, as for core SU 90-24, by linear interpolation between the AMS ^{14}C dates, the position of AZII, and the limit of marine isotope stage 3/4 (Table 2 and Figure 3).

3.3.1. Heinrich events. Amongst the numerous IRD layers observed in core SU 90-24 (Figure 2), five of them have ages analogous to the HE from the midlatitude sediment cores [Andrews and Tedesco, 1992; Bond et al., 1992, 1993; Cortijo et al., 1997; Vidal et al., 1997]. The base, top, and duration of the lithic events in all sediment cores have been determined by reference to the midheight peak of each lithic event.

The IRD layers corresponding to HE₁ have an average age of 15 ± 0.7 ka and an average duration of 1.7 ± 0.7 kyr (Figure 5a

and Table 3). In cores SU 90-24 and SU 90-08 this event shows two lithic peaks.

HE₂ has an average age of 22.2 ± 1.1 ka and a duration of 1.8 ± 1.2 kyr (Figure 5b and Table 3). The comparison of the ages obtained for each lithic layer and the calculated average ages for the base and top of HE₂ shows some small differences. The large standard deviation, above 1 ka, can be mainly attributed to the young age found for the base of HE₂ in core SU 90-08 which has low sedimentation rates and fewer AMS ^{14}C constraints (Figure 3).

HE₃ is poorly defined and is characterized by a different signature when compared to the other events (Figure 5c and Table 3). The presence of an IRD layer at 43°N in core SU 90-

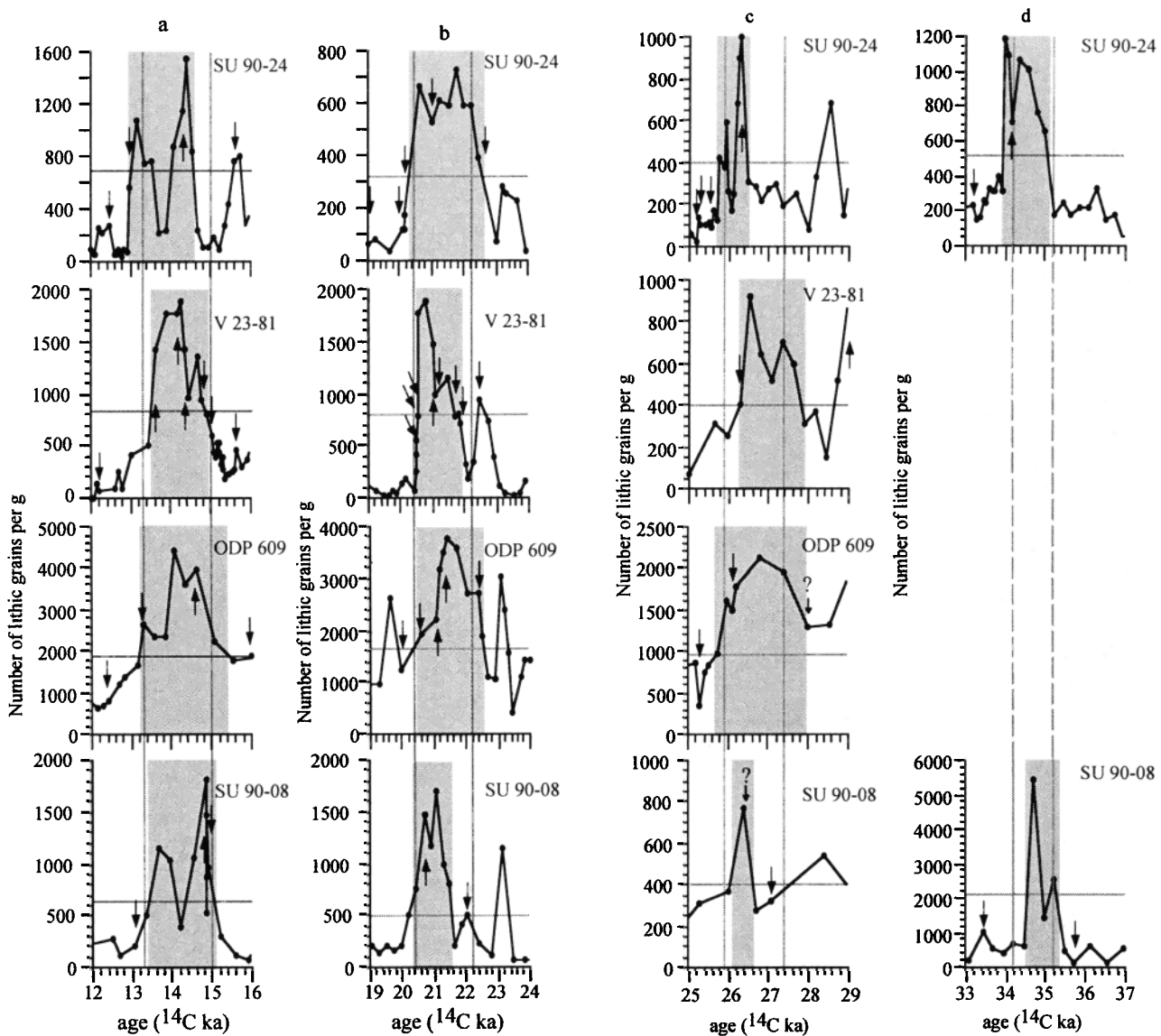


Figure 5. Comparison of the ages of HE₁ to HE₃ from the sediment cores presented in Figure 4: (a) the ice rafted detritus (IRD) content from 12 to 16 ka, HE₁; (b) the IRD content from 19 to 23 ka, HE₂; (c) the IRD content obtained from 25 to 29 ka (from these results the limits of HE₃ are not clearly defined, and this event does not appear to be synchronous throughout the North Atlantic as is the case for the other HE); and (d) the IRD content obtained from sediment cores SU 90-24 and SU 90-08 from 33 to 37 ka, HE₄. The AMS ^{14}C dates used to derive the age of each event are indicated for each record by small arrows, these dates are reported in Table 2. The base and top have been determined by reference to the midheight of the peak lithic value. When the HE was defined by more than one peak, the average was taken. The average age of the top and base of each HE is indicated by solid lines (Table 3).

Table 3. Calculated Average Age of the Base and Top of the Coarse Lithic Layers Corresponding to Heinrich Events (HE₁ to HE₄)

Core	Latitude	Base Age, ka	Top Age, ka	Duration, ka	Thickness, cm
HE ₁					
SU 90-24	62°N	14.6	13.0	1.6	18
V 23-81	55°N	15.0	13.5	1.5	12
ODP 609	50°N	15.4	13.2	2.2	8
SU 90-08	43°N	15.1	13.4	1.7	20
HE ₂					
SU 90-24	62°N	22.6	20.3	2.3	16
V 23-81	55°N	21.9	20.6	1.4	11
ODP 609	50°N	22.6	20.4	2.2	9
SU 90-08	43°N	21.5	20.4	1.1	10
HE ₃					
SU 90-24	62°N	26.5	25.8	0.7	20
V 23-81	55°N	27.9	26.2	1.7	6
ODP 609	50°N	28.0	25.6	2.4	7
SU 90-08	43°N	26.7	26.0	0.7	4
HE ₄					
SU 90-24	62°N	35.1	33.9	1.2	14
V 23-81	55°N	35.2	34.1	1.1	16
ODP 609	50°N	35.3	34.6	0.7	16
SU 90-08	43°N	35.3	34.5	0.8	6

The ages have been determined by reference to the midheight peak. The ages of HE₄ in ODP site 609 and core V 23-81 are indicated but have not been used to calculate the average age and duration because there are no AMS ¹⁴C dates for these events. The average age and duration are as follows: HE₁, 15±0.7 ka and 1.7±0.7 kyr; HE₂, 22.2±1.1 ka and 1.8±1.2 kyr; HE₃, 27.2±1.6 ka and 1.4±1.7 kyr, and HE₄, 35.2±0.3 ka and 1±0.6 kyr.

08 is very speculative, and a higher-resolution study would be necessary. At 50° and 55°N this event corresponds to a period of ~2 kyr duration, but the maximum abundance of lithic grains remains low in comparison with HE₁ and HE₂ (Figure 4). Furthermore, the base and top of these IRD layers may not be accurately defined (Figure 5c). On the contrary, in core SU 90-24, HE₃ corresponds to a period of 700 years with a distinct increase of lithic content. The IRD layer corresponding to HE₃ in the Irminger Basin seems to correspond to the end of the corresponding IRD layer in the midlatitudes. Thus the average age and duration of this event have the largest standard deviation, 27.2 ± 1.6 ka and 1.4 ± 1.7 kyr (Table 3), respectively.

Results from cores SU 90-08 and SU 90-24 give an average age and duration of HE₄ of 35.2 ± 0.3 ka and 1 ± 0.6 kyr (Figure 5d and Table 3), respectively. Although this age has been obtained from only two records, it nevertheless confirms the 35.1 ± 1.1 ka age of HE₄ [Cortijo et al., 1997] and 35.5 ka [Bond et al., 1993]. There are no AMS ¹⁴C dates to constrain the age of HE₄ in the other sediment cores which have been dated by correlation with core SU 90-24.

For HE₅ we are close to the limits of AMS ¹⁴C dating. Nevertheless, in core SU 90-24 the date obtained at 510 cm just below a broad lithic layer is 44.2 ± 2.6 ka (Figures 3 and 4). This age is close to the interpolated age of HE₅ in ODP site 609 [Bond et al., 1993] but must be confirmed as the IRD layer follows a period of AMS ¹⁴C inversions (Figure 3). There are no other available AMS ¹⁴C dates for this particular event in the literature.

3.3.2. The other detrital events. In core SU 90-24, numerous other detrital events (DE) are observed (Figure 2); they show a strong similarity with the lithic events in ODP

site 609 and core V 23-81 (labeled a-h in Figure 4). Bond and Lotti [1995] have correlated each of these lithic cycles with the cold stadials recorded in the Greenland Ice Core Project (GRIP) ice core. In core SU 90-24 the amount of lithics deposited during these events and their duration are similar and sometimes even larger than during the HE, and they cannot be considered as smaller-scale iceberg discharges. The ages of these events may not be easily compared given the small amplitude of some of the IRD layers in the midlatitudes. Nevertheless, a certain number of DE in core SU 90-24 seem to correspond to those previously observed by Bond and Lotti [1995] (Figure 4).

3.3.4. Origin of the lithics. Different families of lithics have been visually distinguished under the binocular in core SU 90-24. The most important fractions are composed of translucent hyaline minerals: quartz and feldspar, diverse rock fragments, and volcanic ash. Two distinct thick layers of translucent rhyolitic glass shards correspond to AZI and AZII (Figure 2). Fresh, unaltered, dark volcanic glass shards compose up to 40% of the total lithic content during most of the IRD events except for a short period, between 90 and 140 cm (Figure 2), which corresponds to the last glacial maximum. The detrital carbonate observed in the Heinrich layers of the sediment cores from the midlatitudes [Bond et al., 1992; Grousset et al., 1993; Bond and Lotti, 1995] in the Arctic Sea [Bischof et al., 1996] and in the Labrador Sea [Andrews and Tedesco, 1992] which is commonly used as an indicator of the Laurentide ice sheet source was not observed in the coarse lithic fraction of core SU 90-24.

4. Discussion

4.1. Origin of the Icebergs

4.1.1. In the Irminger Basin. The presence of fresh basaltic glass in core SU 90-24 indicates that icebergs which delivered their IRD into the Irminger Basin originated at least partly from Iceland (Figure 2). The remaining lithics could be indicating multiple iceberg origin, but a more accurate petrologic study would be necessary. Nevertheless, the absence of detrital carbonate in the Irminger Basin shows that icebergs originating from the northern Laurentide ice sheet which borders the Arctic sea [Bischof et al., 1996] did not undergo important iceberg discharges or that if they did, icebergs did not drift out of the Arctic Sea to the Irminger Basin.

4.1.2. Comparison with the midlatitude sediment cores. In the midlatitudes, there is a clear difference between the HE, with important contribution of detrital carbonate from the Laurentide ice sheet, and the smaller DE, characterized by increased basaltic glass and hematite-coated grains [Bond and Lotti, 1995]. The Laurentide ice sheet thus did not significantly contribute to these other DE.

These observations show that from 10 to 60 ka, successive icebergs discharges originated from the Nordic regions. They first delivered their IRD, rich in Icelandic material, into the Irminger Basin and then drifted into the midlatitudes of the North Atlantic Ocean where they melted entirely. The Laurentide ice sheet seems to have only contributed to the more imposing HE. Furthermore, the initial phase of the coarse lithic layers corresponding to HE₁, HE₂, and HE₄ in ODP site 609

and core V 23-81 is marked by higher percentages of hematite coated grains and fresh basaltic glass [Bond and Lotti, 1995]. The massive iceberg discharges from the Laurentide ice sheet correspond to the upper part of the IRD layers. The deposit of characteristic detrital carbonate then diluted or replaced the other components. Thus, during the HE the first icebergs to reach the midlatitudes of the Atlantic Ocean did not originate from the central Laurentide ice sheet but at least partly from Iceland [Bond and Lotti, 1995].

4.2. Synchronicity of the Iceberg Discharges

4.2.1. The Heinrich events. The ages obtained for the different lithic layers corresponding to HE₁, HE₂, and HE₄ from 42° to 62°N show only some small differences (Figures 4 and 5 and Table 3). No systematic lags or leads or any spatial gradients can be observed. Given the differences in sedimentation rates (Figure 3), the thicknesses of the IRD layers (Table 3), the sampling and AMS ¹⁴C dating resolution, and the effects of bioturbation which smooth and disturb the initial records, the IRD layers corresponding to the HE can be considered approximately synchronous.

In all sediment cores, HE₃ presents a particular signature and does not appear to be synchronous (Figure 5c). Previous studies have shown that HE₃ is believed to have a distinct origin when compared to the other major HE, and the geochemical signature of the noncarbonate lithics deposited during this period also indicates multiple sources and is similar to the background sediment in the area [Grousset et al., 1993; Gwiazda et al., 1996a; Revel et al., 1996]. Nevertheless, detrital carbonate, presumably coming from eastern Canada, is present in what appears to be equivalent to HE₃ on Orphan Knoll,

and a small amount of detrital carbonate also occurs within HE₃ in core V 23-81 [Bond and Lotti, 1995]. It appears that the Laurentide ice sheet may have discharged icebergs at the time of HE₃, but on a much smaller scale than the other HE. Furthermore, by using the more classical method for dating the HE, which refers to the peak concentration of lithics, a common age ~26-26.5 ka can be observed for this particular event in most sediment cores. Therefore the massive iceberg discharges which occurred every 5-10 kyr during the last glacial period known as the Heinrich events originated from the Laurentide ice sheet but also from at least Iceland and perhaps other Nordic regions.

The duration of an average HE has previously been estimated between about 200 and 2000 years [François and Bacon, 1994; Dowdeswell et al., 1995; Thomson et al., 1995; Hulbe, 1997]. Results from this study, based on AMS ¹⁴C dates, show that the ice-rafted debris were deposited over a period of 1-2 kyr. In the 40°-50°N latitudinal range, bioturbation effects could extend the duration of these events as reduced foraminiferal abundance within the lithic layers produces artificially older ages at the base and younger ages at the top of the event [Manighetti et al., 1995]. However, in core SU 90-24 the foraminifera and IRD content increase simultaneously (Figures 2 and 6). Bioturbation should have the opposite effect and artificially give a shorter duration. This is not observed and might indicate that the processes described by Manighetti et al. [1995] do not significantly change the AMS ¹⁴C ages of HE.

4.2.2. The other lithic events. The variability in morphology and thickness of the other "non-Heinrich events", the DE, limits the possibilities of closely comparing their ages on a north-south transect (Figure 4). Nevertheless, a certain number of DE previously observed by Bond and Lotti [1995] appear to be present in core SU 90-24 (Figure 4). Their lithic composi-

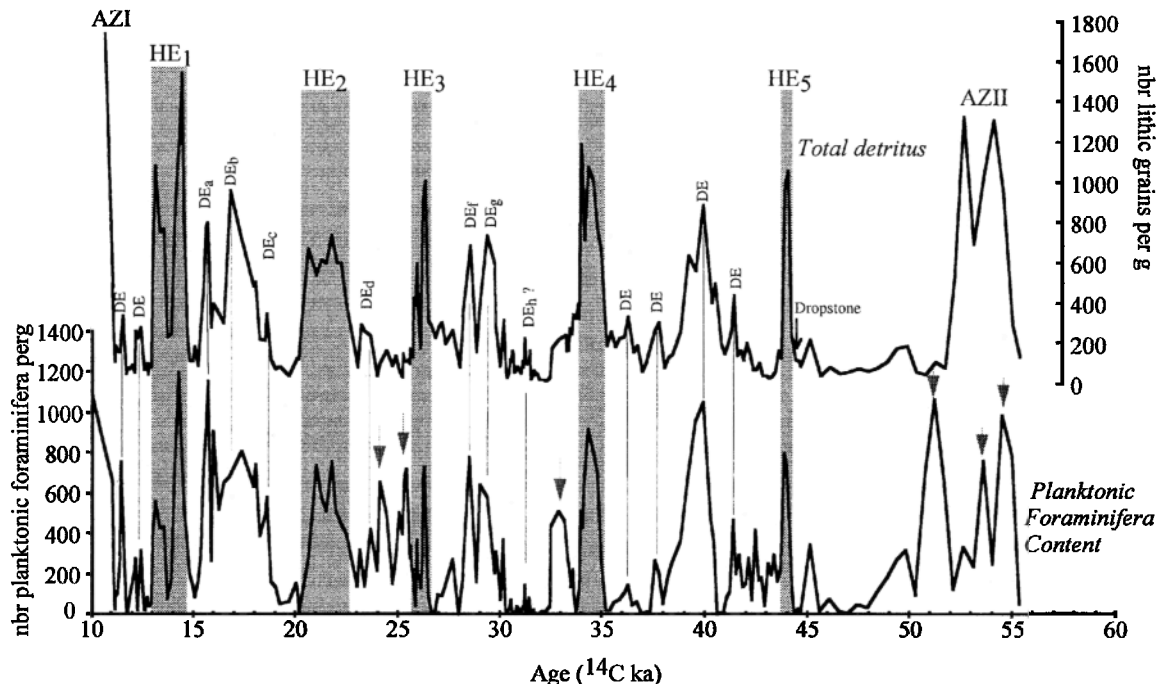


Figure 6. The coarse lithic content and foraminiferal abundance in core SU 90-24 versus age in ka. The positions of HE₁ to HE₅ are indicated by the shadowed intervals. The peak concentration of IRD during the non-Heinrich events, or the detrital events (DE), are indicated by thin lines. At the base of the lithic event corresponding to HE₅ a large dropstone was observed.

tion is also similar in that they are rich in dark volcanic glass at each location. Only one exception can be observed in the Irminger Basin during DE_a to DE_c. This coldest phase of the last glacial period corresponding to MIS 2 was probably characterized by different patterns of sea surface currents and sea ice cover. The absence of volcanic ash at the location of core SU 90-24 may correspond to different iceberg drift paths. Spectral analyses of the lithic content record shows that these DE occur at frequencies between 1.2 and 3.8 kyr. Thus Iceland and the other Nordic ice sheets underwent iceberg discharges on millennium timescales. These have been recorded in core SU 90-24 and in the midlatitudes. Bond and Lotti [1995] as well as Rasmussen et al [1996] considered that these oscillations are directly related to the D-O cycles recorded in the Greenland ice sheet.

There are thus two oscillating systems: long-term iceberg discharges on timescale of 5-10 kyr from the large continental ice sheet, the HE, and the more rapid millennium timescale instabilities of the Icelandic ice sheet and perhaps the other Nordic regions. The most important observation is that these two systems are closely linked because the initial phase of the major HE at 50°N is composed of basaltic glass originating from the Icelandic ice sheet.

4.3. Iceberg Discharges in the Irminger Basin: Environmental Consequences

4.3.1. Impact on the sea surface productivity. In the high latitudes, biogenic carbonate is mainly controlled by the presence or absence of sea ice cover which reduces light penetration, nutrient input, and sea surface productivity as it is observed today in the present Arctic Seas [Carstens et al., 1997]. Thus glacial high-latitude oceans are generally characterized by low concentrations of foraminifera [Kellogg, 1980; Nam et al., 1995]. Nevertheless, within the Arctic seas, high productivity areas have been observed at the sea ice limit [Carstens et al., 1997] or in active polynia regions [Smith and Nelson, 1985]. Large drifting icebergs are also capable of mixing deep nutrient rich waters with the surface waters and thus increasing the sea surface productivity [Sancetta, 1992].

In core SU 90-24, outside the periods of increased ice-rafted material deposit, foraminiferal abundance is extremely low. Conversely, periods of high foraminiferal abundance are associated with increased lithic content (Figure 6). There are only a few exceptions indicated by small arrows between HE₂ and HE₄ and around AZII. A similar observation has previously been reported in a sediment core from the Faeroe-Scotland Ridge which shows an increase of the foraminifera content during the cold stadial events [Rasmussen et al., 1996].

We interpret this record as an indicator of rapid fluctuations of the extent of sea ice synchronous with periods of iceberg discharges during the glacial period in the Irminger Basin. The increased calving rates were accompanied by a retreat of the sea ice bringing the location of core SU 90-24 into sea ice edge conditions and thus increasing the productivity in the surface waters.

4.3.2. Percentage of *N. pachyderma* l.c.: A proxy of polar sea surface temperature. The % *N. pachyderma* l.c. in sediment core SU 90-24 varies between 95% and 100% corresponding to a range of summer SST from 8° to -1°C (Figure 7) [Pflaumann et al., 1996]. Such small faunal variations may not

be easily translated in terms of precise temperature changes. Except for four excursions to warmer temperatures the SST were low in the Irminger Basin from 10 to 60 ka (Figure 2). On the contrary, in the midlatitudes the relative abundance of *N. pachyderma* l.c. from ODP site 609 at 50°N varies from 100% to 10% [Bond et al., 1993]. The comparison of the two records (Figure 8) gives indications on the position of the polar front [Bé and Tolderlund, 1971; Ruddiman, 1977; Bond et al., 1993] at the time of the increased iceberg discharges. The IRD layers corresponding to the HE in core SU 90-24 occur when the polar front was located south of 50°N as indicated by the high abundance of *N. pachyderma* l.c. from 90% to 100% in ODP site 609 (Figure 8). The sudden northward shift of the polar front toward the end of each HE, indicated by the rapid decrease of *N. pachyderma* l.c., reflects the rapid switch to an active thermohaline circulation and is in agreement with model experiments [Paillard and Labeyrie, 1994]. The abrupt warming which marks the end of the HE corresponds to the resumption of the North Atlantic drift suddenly bringing warmer waters into the high latitudes. These observations confirm that iceberg discharges recorded in the Irminger Basin sediments are related to periods of extreme cold sea surface temperatures throughout the North Atlantic Ocean. Consequently, the increased productivity observed during the lithic deposits in the Irminger Basin cannot be attributed to warmer sea surface temperatures.

4.4. Sea Surface Hydrology Variations Associated With Iceberg Discharges

4.4.1. Major light $\delta^{18}\text{O}$ anomalies associated with the HE. In the Irminger Basin the $\delta^{18}\text{O}$ foraminiferal record shows a series of large light anomalies associated with each of the major HE (Figure 8). The ice-rafted material corresponding to HE₂, HE₃, and HE₄ was deposited a few hundred years before the light $\delta^{18}\text{O}$ peak (Figure 8). This lag cannot be explained by an abrupt increase in sediment rate as a result of rapid deposition

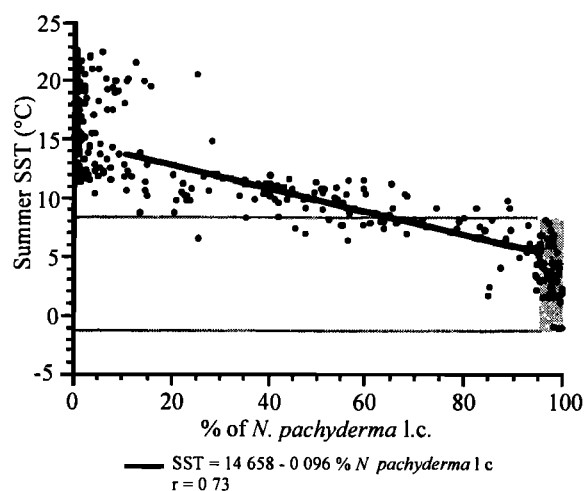


Figure 7. The percentage of *N. pachyderma* l.c. versus summer sea surface temperatures [after Pflaumann et al., 1996]. The % *N. pachyderma* l.c. recorded in core SU 90-24 varies within the shaded interval corresponding to SST ranging from -1°C to 8°C. The linear relationship (heavy line) between the % *N. pachyderma* l.c. and summer sea surface temperatures was calculated for % *N. pachyderma* l.c. only from 10% to 95%.

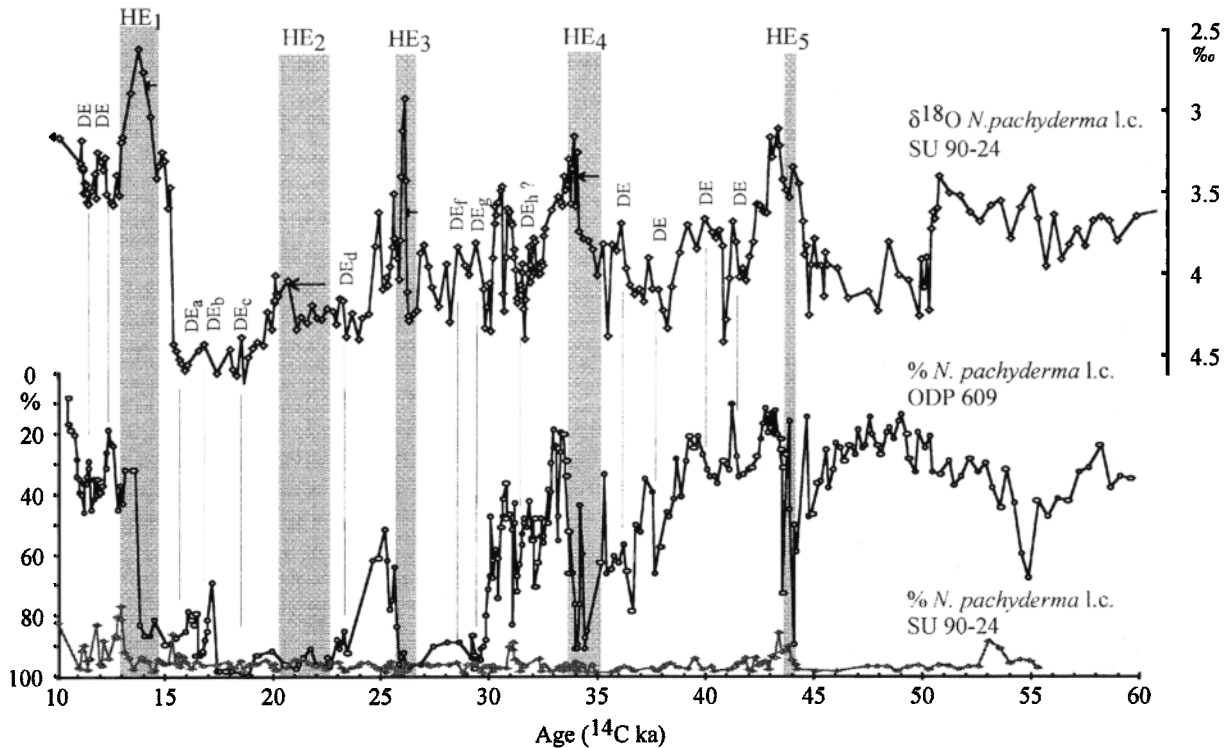


Figure 8. The $\delta^{18}\text{O}$ and the % *N. pachyderma* l.c. records of core SU 90-24 and the % *N. pachyderma* l.c. from ODP site 609 versus age. The shaded intervals correspond to the position of the lithic layers in core SU 90-24 as in Figure 6. The $\delta^{18}\text{O}$ record shows a series of light anomalies which slightly lag the IRD layers corresponding to HE₂, HE₃, and HE₄. The % *N. pachyderma* l.c. from core SU 90-24 is compared to the % *N. pachyderma* l.c. from ODP site 609. The age scales of each core are both constrained by AMS ^{14}C dates from 10 to 30 ka (see Figure 3 and Table 2 for the age scale).

of the ice-rafted lithics because there is no associated decrease in the foraminiferal abundance (Figure 6).

The $\delta^{18}\text{O}$ value of planktonic foraminifera is a function of the temperature of growth [Emiliani, 1955; Shackleton, 1974] and sea surface $\delta^{18}\text{O}$, itself a function of continental ice volume and the sea surface salinity [Emiliani, 1955; Craig, 1965]. In the midlatitude area, HE are associated with major modifications of the relative planktonic foraminiferal abundances and $\delta^{18}\text{O}$ decreases of *N. pachyderma* l.c. This has been interpreted as reduced SST and the $\delta^{18}\text{O}$ negative peaks have been interpreted as the lowering of sea surface salinities [Bond et al., 1992; Bond et al., 1993; Labeyrie et al., 1995; Maslin et al., 1995; Cortijo et al., 1997]. In core SU 90-24 the foraminiferal assemblages are almost entirely monospecific and only show some minor variations between 95% and 100% *N. pachyderma* l.c. (Figure 8). Therefore the light $\delta^{18}\text{O}$ anomalies associated with each HE can be attributed either to an increased SST within the range of polar waters (-1° to 5°C) or to a lowering of the sea surface salinity due to the input of iceberg meltwater.

A close comparison of the IRD content and foraminiferal abundance, oxygen isotope variations, and % *N. pachyderma* l.c. during HE₄ in ODP site 609 and core SU 90-24 shows that these parameters do not vary synchronously (Figure 9). At 50°N the IRD layer is associated with reduced foraminiferal abundance and light $\delta^{18}\text{O}$ values, whereas at 62°N the $\delta^{18}\text{O}$ values remain high and the IRD layer is associated with an

increase in foraminiferal abundance. We postulate that in the Irminger Basin, SSTs were sufficiently low during the iceberg discharges to prevent massive melting. The icebergs probably only released the lithics concentrated at their base and then drifted into the midlatitudes of the North Atlantic Ocean. The main meltwater area for this particular event has been located between 43° - 50°N and 15° - 50°W of the North Atlantic Ocean [Cortijo et al., 1997] well to the south of the Irminger Basin, in agreement with this interpretation. In addition, the high foraminiferal abundance indicates that sea ice had retreated.

The initial phase of reduced $\delta^{18}\text{O}$ values associated with the HE begins when IRD are still being deposited in the Irminger Basin. It is then shortly followed by a decrease of IRD content and foraminiferal abundance (Figure 9). The end of the $\delta^{18}\text{O}$ peak during HE₄ is marked by an increasing foraminiferal abundance (Figure 9). The low $\delta^{18}\text{O}$ values associated with the initial phase are interpreted as evidence of an input of low-saline surface waters subsequently leading to reduced sea surface productivity. The absence of any associated IRD indicates that this low-saline water did not originate locally but corresponds to the northward propagation of iceberg meltwater produced in the midlatitudes. Only the final phase, marked by an increase in the foraminiferal abundance, would correspond to a 2° - 3°C increase in polar water SST (Figure 9). Such a small SST increase would have left the location of the polar front south of core SU 90-24 in agreement with the high

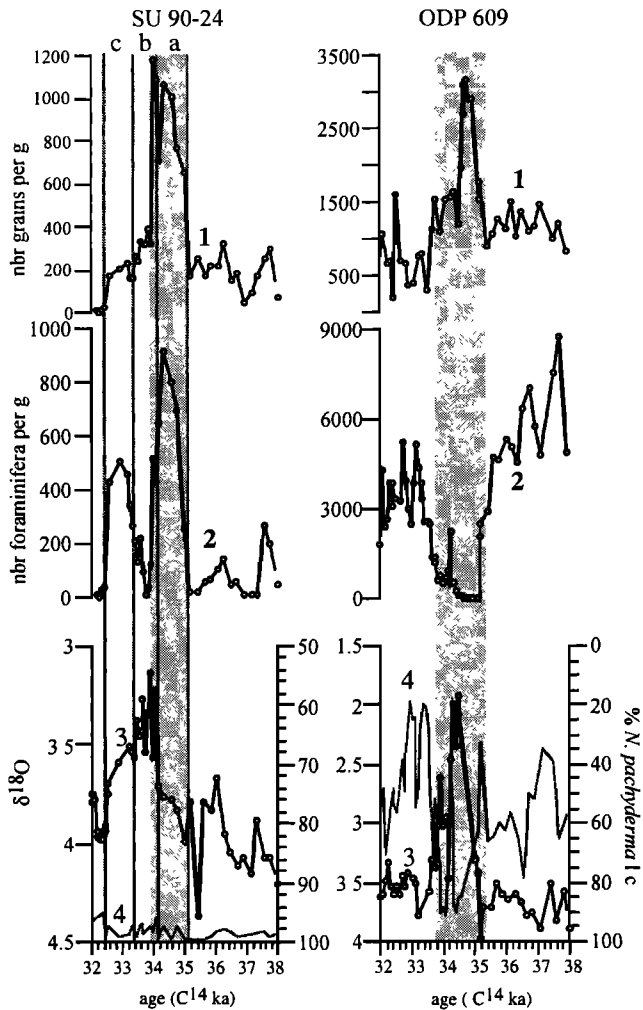


Figure 9. Coarse lithic input, foraminiferal abundance, % *N. pachyderma* l.c., and $\delta^{18}\text{O}$ variations associated with HE₁ in core SU 90-24 (62°N) and ODP site 609 (50°N). Three intervals in core SU 90-24 indicate the succession of events described: a, IRD deposit but no melting in the Irminger Basin, b, initial phase of light $\delta^{18}\text{O}$ interpreted as meltwater input, and c, slight SST increase toward the end of the HE; 1, lithic content in number of lithics (>150 μm) per gram of dry sediment (Figure 5d), and the gray line marks the mid height level in each core as $\delta^{18}\text{O}$ defined in Figure 4, 2, the foraminifera abundance in number of foraminifera per gram of dry sediment, 3, the $\delta^{18}\text{O}$ record from *N. pachyderma* l.c. (open circles), and 4, % *N. pachyderma* l.c.

% *N. pachyderma* l.c. This scenario also applies to HE₂ and HE₃ although there is no increase of the foraminiferal abundance toward the end of HE₂.

In the Irminger Basin, only HE₁ and HE₃ occur in a different context; small decreases of % *N. pachyderma* l.c. toward the end of these events are interpreted as small increases of SST. Furthermore, the deposit of IRD and foraminiferal $\delta^{18}\text{O}$ peaks are synchronous, indicating that there was local melting of icebergs. We suggest that the main meltwater area during these events must have been located further to the north, implying that the polar front was also located further north, closer to the location of core SU 90-24. This could be explained by the general setting in which HE₁ took place, during the deglaciation, and HE₃ occurred during a warmer phase of MIS 3, in comparison with the other HE.

4.4.2. Absence of major $\delta^{18}\text{O}$ anomalies associated with the DE. In the Irminger Basin, as in the midlatitudes [Labeyrie *et al.*, 1995; Maslin *et al.*, 1995; Cortijo *et al.*, 1997], there are no significant changes of planktonic foraminiferal $\delta^{18}\text{O}$ associated with the DE, outside the major HE (Figure 8). Yet some of the IRD layers in core SU 90-24, in particular DE_b, DE_r, and DE_g, present equal and sometimes even larger quantities of lithics as those deposited during the HE (Figure 4). On the Faeroe-Scotland Ridge, Rasmussen *et al.* [1996] have observed distinct light $\delta^{18}\text{O}$ anomalies during each cold stadial, but these are always much smaller in amplitude when compared to those associated with the HE.

Two main processes can influence the signature of melting icebergs on sea surface $\delta^{18}\text{O}$: the rapidity at which icebergs melt and their origin. During each detrital event, low SST in the Irminger Basin would permit only a small amount of iceberg to melt, liberating a limited amount of low $\delta^{18}\text{O}$ meltwater. The amplitude of the $\delta^{18}\text{O}$ anomalies is also controlled by the source of icebergs. Whereas the snow deposited in central regions of large continental ice sheets, away from the ocean and at high altitude, should have rather low $\delta^{18}\text{O}$ values $\sim -40\text{‰}$ versus SMOW, ice from the coastal ice sheets around the Nordic seas was much less fractionated, in the -20‰ range [Dansgaard and Tauber, 1969]. The isotopic signature of icebergs originating from smaller coastal ice sheets could then induce smaller sea surface $\delta^{18}\text{O}$ anomalies. The combined effect of slower melting and of the more proximal source can thus explain the absence of large anomalies associated with the non-Heinrich lithic layers. Conversely, during the major HE the large $\delta^{18}\text{O}$ anomalies correspond to the melting of icebergs which originate from more central regions of the Laurentide ice sheet and perhaps other northern continental ice sheets. This interpretation would explain why only the major HE are associated with drastic reductions of sea surface $\delta^{18}\text{O}$.

4.5. Links Between the Nordic and Laurentide Ice Sheets During the Iceberg Discharges

What is regulating the rapid oscillations of the Nordic coastal ice sheets? The preferential accumulation of snow and ice around the coastal areas of the Nordic regions and in particular around the smaller ice caps which cover the Faeroes and Iceland islands could lead more rapidly to a state of disequilibrium and explain the frequent iceberg discharges from these regions. Recent model results have shown that ice shelves could grow and decay on such millennium timescales [Hulbe, 1997]. The rapid instabilities of the coastal ice sheets and ice shelves would be climatically driven as their growth is dependent on the moisture supply transported at high northern latitudes, which itself is associated with the rate of thermohaline circulation. Large continental ice sheets such as the Laurentide ice cap should also be sensitive to changes in the snow accumulation rates, but the inertia of massive ice cap are such that they would respond on longer timescales. Nevertheless, the presence of hematite-stained grains in midlatitude sediment cores during the more frequent DE and during the initial phase of the HE [Bond and Lotti, 1995] suggests that similar coastal ice sheet and ice shelf instabilities could have affected the area close to the Gulf of St. Lawrence. The southeastern, marine-based, part of the Laurentide ice sheet would thus respond to the same processes as those which

operate in the Nordic regions and oscillate on millennium timescales.

Can these "smaller-scale" iceberg surges trigger such massive collapses of the Laurentide ice sheet? Bond and Lotti [1995] suggested that this could have been the case on the basis of evidence that Heinrich events were always immediately preceded by one of the smaller IRD discharges. In their view the smaller events triggered the collapses of ice in Hudson Strait corresponding to the Heinrich events every 5 to 10 ka. This period reflects the time needed for the large continental ice caps to reach an unstable condition in which another discharge might be triggered [MacAyeal, 1993a; Bond and Lotti, 1995]. Results from this paper are in agreement with such a scenario; the massive HE occur at the end of a series of DE corresponding to instabilities of the coastal ice sheets and ice shelves from the Nordic regions and perhaps also close to the Gulf of St. Lawrence. Small sea level changes would be associated with the instabilities of the coastal ice sheets every 1.2-3.8 kyr. These could facilitate the Laurentide ice sheet collapses if they occurred within the unstable period. The system would be even more efficient if the different marine-based Nordic ice sheets, themselves linked through the regional climatology and sea level, reacted in phase, increasing the amplitude of sea level change associated with each Nordic event.

5. Conclusions

In the Irminger Basin glacial sediments, numerous IRD layers have been observed. They correspond to periods of sudden increases of iceberg discharges which occurred on millennium timescales and originated, at least partly, from the Iceland ice sheet. Equivalent lithic layers can be observed further south in the midlatitudes where they are superimposed by the larger but less frequent IRD inputs from the Laurentide. The rapid growth of the coastal ice caps and ice shelves bordering Iceland, the Faeroe islands, and the other coastal areas of the Nordic regions, onto the marine margins could lead to such frequent iceberg discharges. The synchronous deposit of lithics from different northern hemisphere ice sheets during the Heinrich events indicates that the Laurentide ice sheet was not the only one to contribute to the Heinrich layers. Furthermore, the Laurentide ice sheet discharges corresponding to the Heinrich events seem to be triggered by the more frequent instabilities

from the higher latitudes. This suggests that the continental ice caps were highly sensitive to small sea level variations. However, it is only every 5-10 ka, when these ice sheets have reached a state of disequilibrium, that these sea level changes have significant repercussions on the larger continental ice caps. Our observations therefore suggest that there are two oscillating systems: increased iceberg discharges from the coastal ice sheets and ice shelves in the Nordic area that occur on a millennial scale while the large continental ice caps such as the Laurentide respond on a longer timescale.

The impact of these climatic instabilities on the sea surface hydrology is different in the Irminger Basin and in the midlatitudes of the Atlantic Ocean. The planktonic foraminiferal abundance in core SU 90-24 which is low during most of the glacial period increases during each coarse lithic layer and could be indicative of oscillations of the sea ice limit during coastal ice sheet instabilities and iceberg discharges. Large $\delta^{18}\text{O}$ anomalies are only associated with the HE and seem to present two successive phases. During the initial period of IRD deposit associated with HE₂, HE₃, and HE₄, sea surface $\delta^{18}\text{O}$ remains high, suggesting that SST were too low for icebergs to significantly melt at 62°N. The initial phase of low $\delta^{18}\text{O}$ is interpreted as a northward propagation of meltwater from the midlatitudes which is followed by the second phase of increased sea surface temperatures within the range of the polar waters. Thus the variability of the $\delta^{18}\text{O}$ record reflects the sea surface hydrology modifications associated with the resumption of an active thermohaline circulation. The absence of large $\delta^{18}\text{O}$ anomalies during the other non-Heinrich events, the detrital events, is in agreement with the coastal origin of icebergs characterized by higher values of $\delta^{18}\text{O}$.

Acknowledgments. Basic support from the CEA-CNRS to the CFR, programs Geosciences Marines, DYTEC, PNEDC (INSU), and EU Environment program EV5VCT 920117 and ENV4CT 950131 are acknowledged. The isotopic data were obtained in Gif sur Yvette; B. Lecoat, D. Dole and J. Tessier were in charge of the measurements. H. Leclaire's support and advice for micropaleontology were of great help. We also acknowledge M. Arnold, who is in charge of the Tandetron in Gif-sur-Yvette where the accelerator mass spectrometry ^{14}C dates, presented here, have been obtained. The role of IFREMER and Genavir in operating the coring cruise Paleocimat I of the French R/V *Le Suroit* is acknowledged. The paper has been greatly improved thanks to discussions with M. Paterne, S. Nees, and D. Paillard and reviews by D. Darby, W. Ruddiman, and one anonymous reviewer. This is an LSCE contribution N°129.

References

- Andrews, J. T., and K. Tedesco, Detrital carbonate-rich sediments, northwestern Labrador Sea: Implications for ice-sheet dynamics and iceberg rafting (Heinrich) events in the North Atlantic, *Geology*, 20, 1087-1090, 1992.
- Bard, E., Correction of accelerator mass spectrometry ^{14}C ages measured in planktonic foraminifera Paleooceanographic implications, *Paleoceanography*, 3, 635-645, 1988.
- Bard, E., M. Arnold, and R. G. Fairbanks, ^{230}Th , ^{233}U and ^{14}C ages obtained by mass spectrometry on corals, *Radiocarbon*, 35, 191-199, 1993.
- Bard, E., M. Arnold, J. Mangerud, M. Paterne, L. Labeyrie, J. Duprat, M.-A. Melheres, E. Sonstegaard, and J. C. Duplessy, The North Atlantic atmosphere-sea surface ^{14}C gradient during the Younger Dryas climatic event, *Earth Planet. Sci. Lett.*, 126, 275-287, 1994.
- Bé, A. W. H., and D. S. Tolderlund, Distribution and ecology of living planktonic foraminifera in surface waters of the Atlantic and Indian oceans, in *Micropaleontology of the Oceans*, pp. 105-149, Cambridge Univ. Press, New York, 1971.
- Bischof, J., D. L. Clark, and J.-S. Vincent, Origin of ice-rafted debris: Pleistocene paleoceanography in the western Arctic Ocean, *Paleoceanography*, 11, 743-756, 1996.
- Bond, G., and R. Lotti, Iceberg discharges into the North Atlantic on millennial timescales during the last glaciation, *Science*, 267, 1005-1010, 1995.
- Bond, G., et al., Evidence for massive discharges of icebergs into the glacial North Atlantic, *Nature*, 360, 245-249, 1992.
- Bond, G., W. Broecker, S. Johnsen, J. McManus, L. Labeyrie, J. Jouzel, and G. Bonani, Correlations between climate records from North Atlantic sediments and Greenland ice, *Nature*, 365, 143-147, 1993.
- Broecker, W. S., Massive iceberg discharges as triggers for global climate change, *Nature*, 372, 421-424, 1994.
- Carstens, J., D. Hebbeln, and G. Wefer, Distribution of planktonic foraminifera at the ice margin in the Arctic (Fram Strait), *Mar. Micropaleontol.*, 29, 257-269, 1997.
- Coplen, T. B., Normalization of oxygen and hydrogen isotope data, *Chem. Geol.*, 72, 293-297, 1988.

- Cortijo, E., L. Labeyrie, L. Vidal, M. Vautravers, M. Chapman, J.-C. Duplessy, M. Elliot, M. Arnold, J.-L. Turon, and G. Auffret, Changes in sea surface hydrology associated with Heinrich event 4 in the North Atlantic Ocean between 40° and 60°N, *Earth Planet. Sci. Lett.*, **146**, 29-45, 1997.
- Craig, H., The measurement of oxygen isotope paleotemperatures, in *Stable Isotopes in Oceanographic Studies and Paleotemperatures*, edited by E. Tongiorgi, pp. 161-182, Spoleto, Pisa, 1965.
- Dansgaard, W. and H. Tauber, Glacier oxygen-18 content and Pleistocene ocean temperatures, *Science*, **166**, 499-502, 1969.
- Dansgaard, W., et al., Evidence for general instability of past climate from a 250 kyr ice-core record, *Nature*, **364**, 218-220, 1993.
- Denton, G. H., T. J. Hughes, and W. Karlen, Global ice-sheet system interlocked by sea level, *Quat Res.*, **26**, 3-26, 1986.
- Dowdeswell, J. A., M. A. Maslin, J. T. Andrews, and I. N. McCave, Iceberg production, debris rafting, and the extent and thickness of Heinrich layers (H1, H2) in North Atlantic sediments, *Geology*, **23**, 301-304, 1995.
- Emiliani, C., Pleistocene temperatures, *J. Geol.*, **63**, 538-578, 1955.
- François, R., and M. Bacon, Heinrich events in the North Atlantic: Radiochemical evidence, *Deep Sea Res.*, Part II, **41**, 315-334, 1994.
- Grousset, F., L. Labeyrie, J. Sinko, M. Cremer, G. Bond, J. Duprat, E. Cortijo, and S. Huon, Patterns of ice-rafted detritus in the glacial North Atlantic (40-55°N), *Paleoceanography*, **8**, 175-192, 1993.
- Gwiazda, R. H., S. R. Hemming, and W. S. Broecker, Provenance of icebergs during Heinrich event 3 and the contrast to their sources during other Heinrich episodes, *Paleoceanography*, **11**, 371-378, 1996a.
- Gwiazda, R. H., S. R. Hemming, and W. S. Broecker, Tracking the sources of icebergs with lead isotopes: The provenance of ice-rafted debris in Heinrich layer 2, *Paleoceanography*, **11**, 77-93, 1996b.
- Heinrich, H., Origin and consequences of cyclic ice-rafting in the northeast Atlantic Ocean during the past 130000 years, *Quat Res.*, **29**, 142-152, 1988.
- Hulbe, C. L., An ice shelf mechanism for Heinrich layer production, *Paleoceanography*, **12**, 711-717, 1997.
- Hut, G., Stable isotope reference samples for geochemical and hydrological investigations, report to the Director General, Int. At. Energy Agency, Vienna, 1987.
- Kellogg, T.B., Paleoclimatology and paleoceanography of the Norwegian and Greenland seas: Glacial-interglacial contrasts, *Boreas*, **9**, 115-137, 1980.
- Labeyrie, L., et al., Surface and deep hydrology of the northern Atlantic Ocean during the past 150 years, *Philos. Trans. R. Soc. London*, **348**, 255-264, 1995.
- MacAyeal, D. R., Binge/Purge oscillations of the Laurentide Ice Sheet as a cause of the North Atlantic's Heinrich events, *Paleoceanography*, **8**, 775-784, 1993a.
- MacAyeal, D. R., A low-order model of the Heinrich event cycle, *Paleoceanography*, **8**, 767-773, 1993b.
- Manighetti, B., N. I. McCave, M. Maslin, and N. J. Shackleton, Chronology for climate change: Developing age models for the Biochemical Flux Study cores, *Paleoceanography*, **10**, 513-525, 1995.
- Martinson, D. G., N. G. Pisias, J. D. Hays, J. Imbrie, T. C. Moore, and N. J. Shackleton, Age dating and the orbital theory of the ice ages: Development of a high-resolution 0 to 300,000 year chronostratigraphy, *Quaternary Research*, **27**, 1-29, 1987.
- Maslin, M. A., N. J. Shackleton, and U. Pflaumann, Surface water temperature, salinity, and density changes in the NE Atlantic during the last 45,000 years: Heinrich events, deep water formation, and climatic rebounds, *Paleoceanography*, **10**, 527-544, 1995.
- Nam, S., R. Stein, H. Grobe, and H. Hubberten, Late Quaternary glacial-interglacial changes in sediment composition at the east Greenland continental margin and their paleoceanographic implications, *Mar. Geol.*, **122**, 243-262, 1995.
- Paillard, D., and L. D. Labeyrie, Role of the thermohaline circulation in the abrupt warming after Heinrich events, *Nature*, **372**, 162-164, 1994.
- Pflaumann, U., J. Duprat, C. Pujol, and L. Labeyrie, SIMMAX, a modern analog technique to deduce Atlantic sea surface temperatures from Planktonic foraminifera in deep sea sediments, *Paleoceanography*, **11**, 15-35, 1996.
- Rasmussen, T. L., E. Thomsen, C. E. Tjeerd, T. C. E. van Weering, and L. D. Labeyrie, Rapid changes in the surface and deep water conditions at the Faeroe Margin during the last 58,000 years, *Paleoceanography*, **11**, 757-771, 1996.
- Revel, M., J. A. Sinko, and F. E. Grousset, Sr and Nd isotopes as tracers of North Atlantic lithic particles: Paleoclimatic implications, *Paleoceanography*, **11**, 95-113, 1996.
- Ruddiman, W. F., North Atlantic ice-rafting: a major change at 75,000 years before the present, *Science*, **196**, 1208-1211, 1977.
- Ruddiman, W. F., and L. K. Glover, Vertical mixing of ice-rafted volcanic ash in North Atlantic sediments, *Geol. Soc. Am. Bull.*, **83**, 2817-2836, 1972.
- Ruddiman, W.F., and A. McIntyre, The North Atlantic ocean during the last deglaciation, *Palaeogeogr., Palaeoclimatol., Palaeoecol.*, **35**, 145-214, 1981.
- Sancetta, C., Primary production in the glacial North Atlantic and North Pacific Oceans, *Nature*, **360**, 249-251, 1992.
- Shackleton, N. J., Attainment of isotopic equilibrium between ocean water and the benthonic foraminifera genus *Uvigerina*: isotopic changes in the ocean during the last glacial, in *Les Méthodes Quantitatives d'Étude des Variations du Climat au Cours du Pléistocène*, edited by J. Labeyrie, pp. 203-210, Cent. Nat. de la Rech. Sci., Paris, 1974.
- Smith, W. O., and D. M. Nelson, Phytoplankton bloom produced by a receding ice edge in the Ross Sea: Spatial coherence with the density field, *Science*, **227**, 163-166, 1985.
- Thomson, J., N. C. Higgs, and T. Clayton, A geochemical criterion for the recognition of Heinrich events and estimation of their depositional fluxes by the ($^{230}\text{Th}_{\text{excess}}$)₀ profiling method, *Earth Planet. Sci. Lett.*, **135**, 41-56, 1995.
- Vidal, L., L. D. Labeyrie, E. Cortijo, M. Arnold, J. C. Duplessy, E. Michel, S. Becqué, and T. C. E. van Weering, Evidence for changes in the North Atlantic Deep Water linked to meltwater surges during the Heinrich events, *Earth Planet. Sci. Lett.*, **146**, 13-27, 1997.

G. Bond, Lamont-Doherty Earth Observatory, Rt 9W, Palisades, NY 10964.

E. Cortijo, J.-C. Duplessy, M. Elliot, L. Labeyrie, and N. Tisnerat, Laboratoire des Sciences du Climat et de l'Environnement, Laboratoire mixte CNRS-CEA, Av. de la Terrasse, 91198 Gif-sur-Yvette, France. (e-mail: eliot@lsce.cnrs-gif.fr)

J.-L. Turon, Département de Géologie et Océanographie, CNRS Unité de Recherche Associé 197, Avenue des Facultés, 33405 Talence Cedex, France.

(Received October 8, 1997;
revised May 27, 1998;
accepted May 28, 1998)